Instrumentation for Diagnosis of Keratoconus

6

Francesco Versaci and Gabriele Vestri

The current methods to detect, diagnose, and monitor the evolution of keratoconus morphologically are computerized videokeratoscopy, corneal tomography, and optical scanning tomography, both in the Scheimpflug configuration as well as based on optical coherence. For reference, a more detailed list would also include tools based on rasterstereography, Moiré interferometry, or laser interferometry [1, 2] but many of these instruments have remained at the prototype stage, and others have been used only in laboratory for research purposes.

The advent of computerized corneal topography has made it possible to gather considerable information about the shape and refractive behavior of the cornea affected by keratoconus. By means of some of these examination techniques it is also possible to measure both the shape of the front surface as well as the back surface thereby giving more accurate information about the location and shape of the cone, the extension of ectasia, and the refractive power localized in the ectatic area.

In-depth knowledge of the profile of the corneal surface is not only essential in the diagnosis or treatment of keratoconus but it is important in many other aspects of clinical practice. In fact, since the cornea alone is responsible for about 80 % of the refractive power of the eye [3], its form has extreme importance in the study of visual function: this surface, formed by the front face of the cornea and coated by the tear film, presents, in fact, the highest refractive index jump with respect to all other elements of the dioptric ocular system and small changes of its shape produce considerable effects on the optical quality of the entire ocular system. Therefore, a careful study of the corneal morphology, in addition to providing valuable information in the early diagnosis of all corneal diseases that change the shape of the surface (and first keratoconus), lends itself to many other clinical applications such as preoperative planning and postoperative assessment throughout the range of refractive surgery and keratoplasty, the application of rigid contact lenses, or the calculation of intraocular lenses in accordance with the formulas or other methods of calculation.

6.1 Videokeratoscopes

The study of the Purkinje–Sanson image dates from the mid-1800s and was the first method of investigation of catoptric images for diagnostic purposes. A Placido disk (consisting simply of a series of concentric black and white circles with a positive lens in the center) was used to observe

F. Versaci, M.S.E. (✉) • G. Vestri, M.S.E.
CSO srl, Via degli Stagnacci 12/E, Badia a Settimo, Firenze, Italy
e-mail: F.Versaci@csoitalia.it; G.Vestri@csoitalia.it

© Springer International Publishing Switzerland 2017

J.L. Alió (ed.), *Keratoconus*, Essentials in Ophthalmology, DOI 10.1007/978-3-319-43881-8_6

the appearance of images reflected from the corneal surface and evaluate approximately and qualitatively, on the basis of the deformation of the reflections of the circles, aberrations borne by the cornea as shown in Fig. 6.1.

The objective measurement of the radius of curvature of the anterior surface of the cornea, also through mire projected on the cornea and reflected by it, dates back to 1854 [4]. Assuming known dimensions of an object (mires) and its distance from the specular surface (cornea), measuring the size of the images formed by the mirror and applying the catadioptric laws, the shape of the specular surface that has reflected upon is obtained: this principle is based on the elementary keratometry measurement.

It is already clear from this brief history that reflection-based devices or videokeratoscopes do not directly measure the elevation data of the cornea, but rather analyze the physical phenomenon that occurs on the anterior corneal surface: specular reflection.

6.2 The Sagittal Curvature

Conceptually, we can consider modern videokeratoscopes as a derivative of ophthalmometers, so much so that the first method developed in this regard is based on the same principles of the ophthalmometer [5]. Indeed, we can consider a topographic measure as many keratometries with ever larger fixed mires, centered on the same axis. The corneal curvature so measured is called the *sagittal* (or *axial*) curvature and can be defined as the radius of an arc of a circle, centered on the optical axis of videokeratoscope (or the keratometer) when this is well aligned to the corneal vertex, which has the same tangent as the cornea to the point concerned, as shown in Fig. 6.2 on the left. In the branches of topography this measure was carried out essentially for comparison: once the device has been calibrated by acquiring spheres (calibration spheres) with known curvature, the curvature of a sample is estimated by comparing the position of the mires reflected by its surface and the ones obtained from the calibration spheres [6].

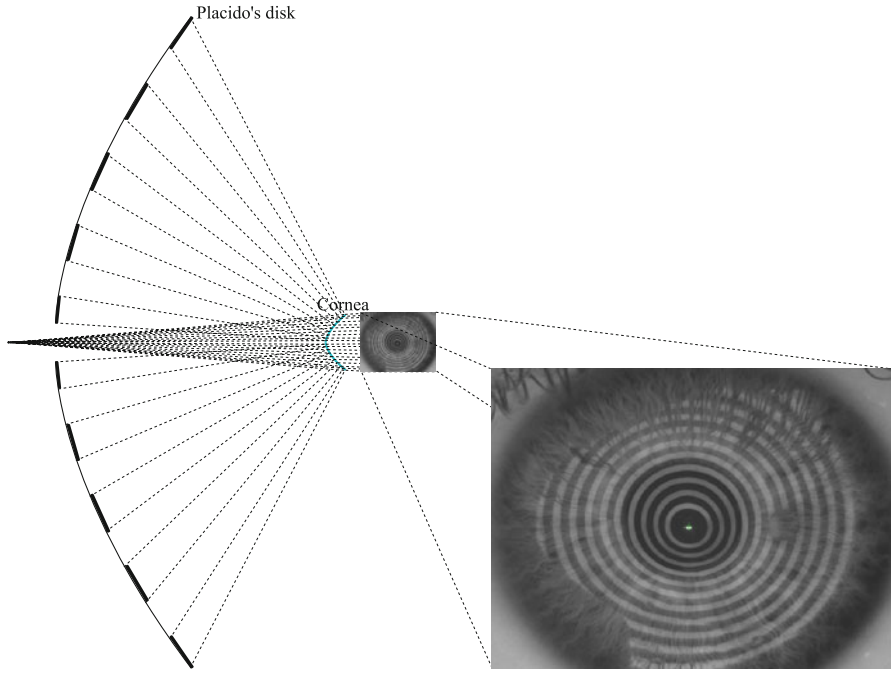

Fig. 6.1 Process of formation of the first Purkinje image from a Placido disk

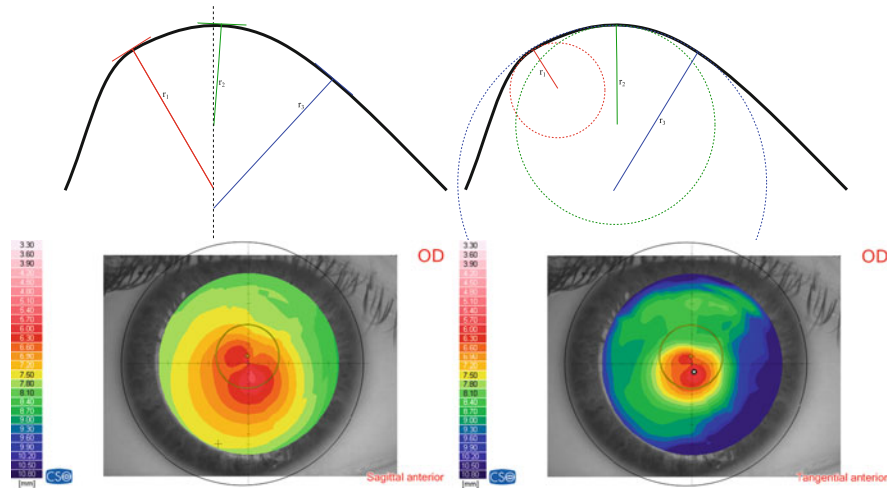

Fig. 6.2 *Left map* of sagittal curvature, *right map* of tangential curvature

The curvature as defined earlier suffers from a low sensitivity for determining shape variations localized in the peripheral cornea. A map of sagittal curvature expressed in diopters, while not being the direct expression of the real refractive power, can represent quite well the optical characteristics of the corneal surface, but it is not able to accurately describe the morphological aspects of the cornea. For this reason, it is felt necessary to support the sagittal curvature with magnitudes which best show the details of the shape of the corneal surface.

6.3 The Tangential Curvature

The *tangential curvature* (sometimes called *instantaneous* or *local*) is the geometric unit that describes the steepening of the cornea, for a given point and in a given direction: it is therefore defined as the radius of the osculating circle for each point belonging to the meridian in question, as shown in Fig. 6.2 on the right. Unlike the sagittal curvature, the center of tangential curvature is not constrained to lie on a reference axis: this condition does not occur unless the cornea is not exactly spherical, and the tangential and the sagittal curvatures are different at every point and coincide only at the vertex. The tangential curvature of a surface is independent of the position of the reference axis along the meridian considered: its sagittal curvature is instead a function of this axis.

6.4 The Height Maps

Topographic maps that represent elevation data are probably more understandable, since they are similar to those used in geographic cartography to describe the elevations of the Earth's surface or the depth of the seabed. The corneal elevation maps are expressed in microns [μm] the position of each point of the cornea, in terms of the elevations along the z axis, with respect to a reference surface. As in geographic maps, where the reference surface is the mean sea level (the *geoid*), the elevation of the corneal surface needs to be expressed in respect to some reference surface: usually spherical, aspherical, or asphero-toric. The reference surfaces, with respect to which the height is measured, are almost always the best-fit surfaces (best approximating surfaces in the sense of the least square error) and have some parameters that characterize them: the spheres are defined by their radius of curvature, the aspherical surfaces by the apical radius of curvature and eccentricity, the asphero-toric surfaces by the apical radius of curvature, eccentricity, and by toricity, that is, the difference of curvature

of the flattest apical meridian and the steepest one. If even one of these parameters is changed, it alters the reference surface and consequently the relative heights of the cornea under examination with respect to it. For this reason, the parameters defining the reference surface are critical to the interpretation of the height map.

6.5 Arc Step

In recent generation reflection-based topographers, tangential curvature, sagittal curvature, elevations, and normals to the surface are calculated simultaneously by a process called *arc step* [7–10]. For videokeratoscopies, the definition of this algorithm marked a real turning point, expanding the range of measurements possible, from only the sagittal curvature to all the morphological or refractive measurements arising from the shape of the cornea.

The arc-step algorithm is summarized as follows: for each point corresponding to the edge of a ring of each meridian, a ray-tracing procedure is carried out, which, from the known positions of the rings on the Placido disk and the detected positions of the keratoscopy rings, allows to derive normals of the surface to be measured. Such information depends on the correct positioning of the surface to be measured and the exact knowledge of the location of the rings of the Placido disk: the first condition is obtained by different methods (maximum sharpness algorithms on a focusing video stream, triangulations, or interruptions of light beams), while the second is known from construction data and is refined by means of instrument calibration. Once the normals to the corneal surface are known (and therefore its derivatives) an iterative algorithm is started. At step 0, the condition of zero derivative in correspondence of the corneal vertex is imposed and, setting the validity of the law of reflection for the first ring, an arc that meets the slope conditions is identified. The algorithm of arc step, as the name suggests, is iterative, and therefore cannot proceed without the knowledge of data obtained in the previous step (step $i-1$) to derive data for the current step (step i). Knowing the coordinates and the normal of $(i-1)$th point, and the normal to the ith point, the coordinates of the new point are determined, by setting conditions of differentiability (surface continuity and continuity of tangency). The reconstructed curve, repeating the pattern shown earlier for all the rings is continuous with continuous first derivative. The connecting functions are circular arcs in the traditional algorithm but can also be polynomial splines or conic arcs (by virtue of their greater flexibility in pursuing the corneal slope). There are essentially two limits in these reconstructions methods and are negligible compared to the advantages they offer:

- Assuming a continuous curve with a continuous derivative is not able to describe steps or cusps (interruption or discontinuity of the derivative). However, it can be reasonably admitted that stroma rarely has discontinuities that cannot be smoothed by the epithelium.
- Separating in fact the reconstruction for each hemi-meridian it is assumed that the normal belongs to the plane on which lays the hemi-meridian itself. This approximation is called *skew ray error* and was thoroughly discussed in the literature [11].

6.6 Optical Scanning Devices

The optical scanning instruments directly measure the sagittal height of the front surface and the back of the cornea (i.e., the corneal elevation with respect to a reference plane). Usually, the transverse field of view goes from limbus to limbus and the vertical is such as to include the entire anterior chamber limited by the iris and the visible part of the lens. The big advantage of this class of instruments is therefore, in addition to the high transverse coverage, the ability to view and measure the whole anterior chamber and all its surfaces (front cornea, posterior cornea, iris, and lens).

The optical scanning devices base their operation on the projection of beams or light slits which, due to scattering effects, diffuse in every direction part of the energy of the incident light.

Therefore, thanks to the scattering, the tissue crossed behaves like a real extended emitter: part of the back-diffused light radiation is captured by a suitable optics able to form the image on the CCD.

6.7 Corneal Thickness

The measurement of the two front and rear corneal surfaces allows agile deduction of pachymetry information: it is the measurement in microns of the distance between the front surface and posterior surface in the direction normal to the anterior corneal surface. It is very useful information from the clinical point of view: it can allow, for example, to assess the evolution of keratoconus or to decide whether a patient may undergo refractive surgery and what can be the maximum amount of the bearable correction of the cornea. In contact lens practice, differential pachymetry can also highlight possible edematous conditions due to the wearing of contact lenses.

6.8 Scheimpflug Camera

The simplest and most intuitive way to obtain the image of a corneal section is to project a luminous slit along a meridional plane of the cornea and to shoot the backscattered light through suitable optics, having its axis of at 90° with respect to this plane and its focus on the plane of the slit (Fig. 6.3 left). This configuration, however, in practice does not work because of obstacles to the path of the shot such as the nose or eyelids. These obstacles force the choice of a nonorthogonal axis of shot to lighting plane and consequently to have a good part of the image out of focus. The Scheimpflug method (see Fig. 6.4) is useful in this case (or Carpentier, or should we say by Scheimpflug's [12] own admission) that shows how to tilt the CCD in order to focus a plane inclined to the axis of the optical system shoot, as shown in Fig. 6.3 on the right. Once scanned the first image, the light blade and the Scheimpflug system can be rotated in order to acquire images of a succession of equidistant angular sections that allow to completely map the anterior segment of the eye. The anterior corneal surface is determined by identifying its edge on the image in section and correcting the distortion effect due to the optical configuration. The internal structures (posterior corneal surface, iris, angles) are determined by identifying the corresponding edges on images in section, correcting the effect of distortion due to the optics in Scheimpflug configuration and correcting the distorting effect given by the fact that they are seen through the overlying corneal surfaces.

- As previously mentioned this technology presents the substantial advantages of a wide coverage of the area measured and the possibility to extend the topographic analysis to the back surface. In considering real corneas meet however important limitations: sectioning the cornea in radial directions and not considering the azimuthal component, the optical scanning systems are also implicitly affected by skew ray error.
- The time required to scan is relatively long (approximately 1 s in the modern conception devices), and then there is the possibility of introducing errors due to the microsaccadic eye movements of the eye examined. Some systems use software corrections for realignment of the acquired sections to overcome this problem.
- The presence of nonperfectly transparent areas of the corneal tissue (such as a scar or opacity) produces a phenomenon known as hyper-backscattering of a certain area of the cornea. This results in the recognition of a false edge and an error in the measurement of the surface.
- These instruments directly measure the elevations, from which it is then possible to deduce mathematical derivation for the curvatures and the refractive data of the cornea: the resolution that can be achieved with this method, however, is significantly lower than that which can be achieved with reflection devices. For this reason, in the majority of cases manufacturers provided a hybrid Scheimpflug + Placido system, allowing a direct measurement of the curvatures of the anterior corneal surface.

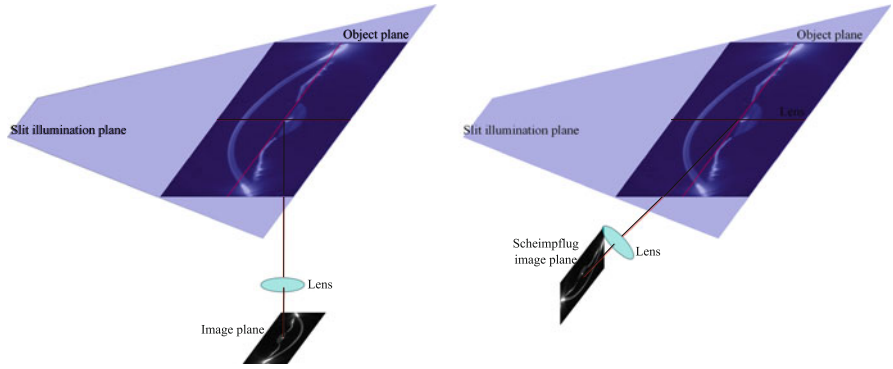

Fig. 6.3 *On the left,* an image system of a section of the cornea with the shooting plane parallel to the plane of illumination. *On the right*, an image system of a section of the cornea in Scheimpflug configuration

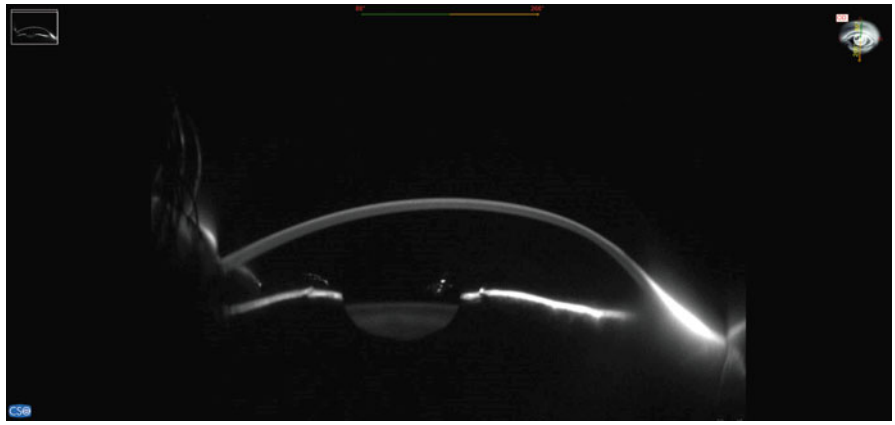

Fig. 6.4 Image of the corneal section of a cornea affected by pellucid obtained by Scheimpflug technology

6.9 AS-OCT (Anterior Segment Optical Coherence Tomography) [13]

Until now, optical tomography coherence has been applied with great success in ophthalmology for the study of the retina and for the measurement of the ocular distances, firstly of the axial length. Only recently industries have turned their attention to this for topography and tomography of the anterior segment of the eye. The reasons for this delay are to be found mainly in the complexity of this technology that is reflected at least for now in high prices of products, in their robustness, in the difficulty of obtaining images that contain the anterior segment in its entirety, and in the difficulty of obtaining accurate measurements comparable to those typical of the simplest techniques in spite of the promising quality of the images.

Optical tomography coherence is a technology based on the measurement of the interference of two beams of broadband radiation (typically infrared) from a reference arm and a sample arm [14–17].

In its simplest embodiment, the radiation emitted from a broadband source, usually an infrared super luminescent diode, is sent in part to a reference arm and in part to a sample arm. A mirror is placed at the end of the reference arm that reflects the beam back toward a fourth arm (detection arm) on which is placed a photodetector. Instead, the radiation sent to the arm of the

sample is backscattered by the ocular tissues and also toward the detection arm, where it interferes with the return beam from the reference arm. If the reference mirror is moved, thereby altering the length of the reference arm, the interference due to the ocular structures encountered by the incident beam of the sample arm can be sampled at various depths. In practice, the photodiode reveals a peak signal at each backscattering element encountered by the beam incident on the sample at a position corresponding to that of the movable mirror of the reference arm.

This type of embodiment is that of the Time Domain OCT (TD-OCT) and is shown in Fig. 6.5a. It was the first to be applied in the field of ophthalmology for the measurement of distances, in particular the axial length of the eye and interdistances between the various ocular structures (thickness of the cornea, the anterior chamber height, thickness of the crystalline lens, etc.). Having this technique the need to move the reference mirror for obtaining a response from the structures at various depths, it presents the speed limit when it is necessary to make a scan of several contiguous axes (A-scan) to create an image of an ocular section (B-scan): eye movements during a slow scan lead to an unwanted and uncorrectable distortion of the scanned image.

A more complex implementation is that which goes under the name of Fourier Domain OCT (FD-OCT) [18], which eliminates the need of scanning the reference mirror to have a measurement at various depths. This allows for the possibility of acquiring slice images relatively quickly, thereby reducing artifacts due to eye movements. The Fourier Domain OCT, in addition to decreasing the time of acquisition, also presents advantages in terms of signal-to-noise ratio compared to the Time Domain. The basic idea is to measure the spectral interference between the radiation returning from the reference arm and the sample arm in a certain range of wavelengths emitted by the source. This means that each wavelength obtains an interference value of the return radiation by the two arms (sample and reference arms) in a single A-scan. The set of these values at various wavelengths is processed with more or less complicated algorithms, but basically containing a Fourier transformation, to obtain the profile of the reflectivity of the sample acquired along an axis.

The Fourier Domain OCT devices are in turn classifiable into the following two classes depending on how they get the interference at various wavelengths: Spectral Domain OCT (SD-OCT in Fig. 6.5b) and Swept Source OCT (SS-OCT in Fig. 6.5c).

The first class of instruments uses a source that emits a certain range of wavelengths all at the same time. The detection arm contains a spectrometer or a device suitable to decompose the returned signal from the sample and reference arms in their components at various wavelengths. In only one stroke the sensor of the spectrometer collects the spectrum necessary, after a sequence of processing, to determine the profile of reflectivity along an axis of the sample. An example of what is achieved with this technology is shown in Fig. 6.6.

The second class of devices uses instead a light source that is a tunable laser, i.e., laser whose wavelength can be changed very quickly [19]. This laser is driven so as to emit in sequence the various wavelengths and is synchronized with a photodiode, which replaces the spectrometer on the detection arm. A processor, which knows the wavelength emitted by the source associates the value measured by the photodiode, and reconstructs in a certain time interval the interference spectrum between the beams coming back from the reference arm and the sample arm.

6.10 Brief Introduction to Automated Systems for Keratoconus Screening

6.10.1 Objective Parameters for Quantifying the Ectasia

The first step toward the creation of systems for the recognition of keratoconus has been dictated by the need to objectify and quantify the morphological distortions caused by the onset of ectasia. Quantitative indicators may in fact exceed the

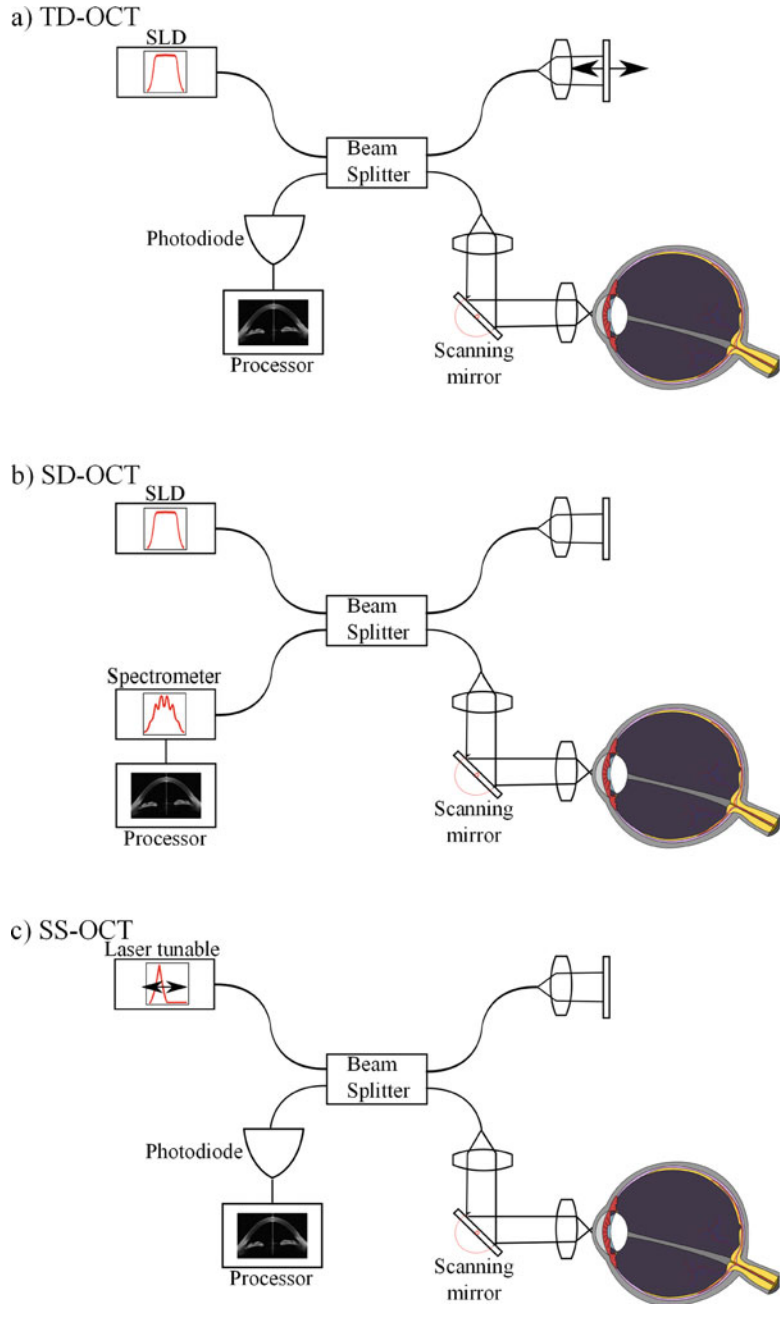

Fig. 6.5 (**a**) Time domain OCT, (**b**) spectral domain OCT, (**c**) swept source OCT

limits of a purely subjective and qualitative interpretation of the topographical framework of a cornea. The calculation of indices also makes possible the temporal interpretation of a case through the comparison of these parameters in the follow-up of the patient: it is in fact possible to monitor over time even very slight variations, so as to keep under observation in a detailed manner the evolution of the pathology.

Since the dawn of modern corneal topography, different authors have proposed different quantitative methods to represent the videokeratoscopic characteristics of keratoconus. The changes induced by the onset of a cone can be

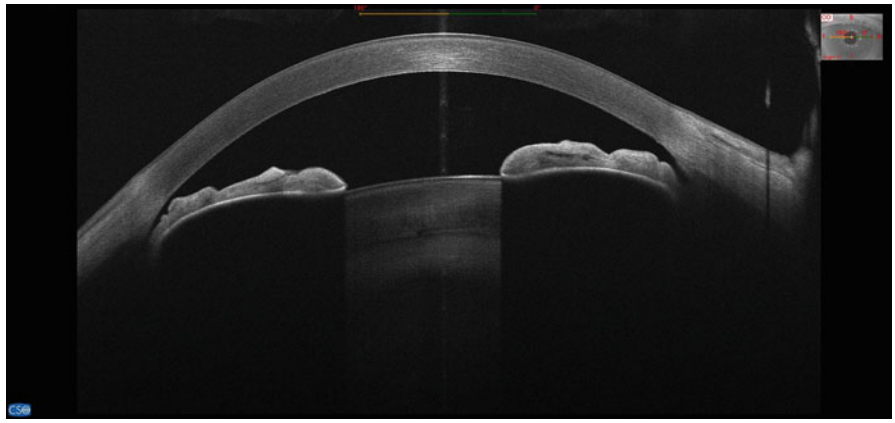

Fig. 6.6 Image of the corneal section of a healthy cornea obtained by technology ASOCT in configuration spectral domain

observed considering wide range of parameters derived from multiple morphological and refractive aspects.

Since the analysis of the anterior surface of the cornea is prior to that of the entire anterior segment, and given that the first topographers provided only sagittal data, the first screening systems for keratoconus and the first indices are based on the analysis of sagittal curvatures of the cornea front: quantitative descriptors derived mainly from sagittal data, such as the KISA% index proposed by Rabinowitz et al. [20–22], the Cone Location and Magnitude Index (CLMI) proposed by Mahmoud et al. [23], and the Keratoconus Prediction Index (KPI) and Keratoconus Index proposed by Maeda et al. [24, 25], have been and are being widely used for keratoconus detection.

Given the desirable characteristics of the tangential curvature in the representation of the shape of keratoconus some authors have abandoned the sagittal representation in favor of the more sensitive tangential representation. Calossi [26] developed some indices derived from the tangential curvature to determine the likelihood of compatibility with a topographic pattern of keratoconus, considering the symmetry and the change of curvature in the ectatic area.

Other indices based on decomposition into Zernike polynomials of the anterior surface of the cornea have been proposed by Schwiegerling and Greivenkamp [27] (Z3 index) and Langenbucher et al. [28], essentially the maps of elevation of a group of healthy patients and a group of patients with the cornea affected by keratoconus have been decomposed into a set of Zernike polynomials and the coefficients resulting from the fitting were compared. The statistical comparison showed that the coefficients that mainly discriminate healthy eyes from keratoconus are those of the third order, $c_3^{\pm 1}$ and $c_3^{\pm 3}$.

Posterior corneal curvature and pachymetry data provided by Scheimpflug imaging have been investigated by Ambrósio et al. [29], who showed that corneal-thickness spatial profile, corneal-volume distribution, percentage increase in thickness, and percentage increase in volume were different in keratoconus and normal eyes. Measurements obtained from the posterior corneal curvature using a Scheimpflug camera have been evaluated in several other papers [30, 31].

6.11 Modern Hybrid Systems Based Assisted Learning

The recognition of keratoconus by its morphological features is a daunting and challenging task and, given that there is no gold standard for the certainty of keratoconus and that there is no agreement on what the signs of topographic lows are, the interpretation of topographical frameworks is often subjective. In addition, if on the one hand modifications induced by the onset of a

cone are such and so many that they can be observed considering a number of parameters resulting from multiple aspects both morphological and refractive, on the other, keratoconus shows itself in forms so different and heterogeneous that only one class of indices is not often enough to ensure its correct diagnosis and description. The combination of such parameters and the weight to be assigned to each of them is often so complicated that many authors, in order to take into account all the heterogeneous variables related to the presence of a corneal ectasia, thought of making use of assisted learning techniques and actually abstracting the problem of classification [24, 25, 28, 32, 33].

Assisted learning itself is a multidisciplinary field: it bases its roots on the results of studies in fields such as artificial intelligence, probability and statistics, computational complexity theory, information theory, and neurobiology. The main objective of a system based on assisted learning is actually to learn to automatically recognize complex patterns and make intelligent decisions based on data provided in a first stage (training) producing useful behavior (or in our case a correct classification) for new cases. Nowadays, we are not yet capable of reproducing automatic learning systems similar to that of humans. However, effective algorithms were invented for certain types of learning tasks.

In the field of classification patterns of corneal topography and recognition of frameworks of keratoconus, three types of systems have been mainly used: decision trees, artificial neural networks, and support vector machines [34, 35]. The first method is a method of learning in which the element that learns is representable by a set of rules if-else. An artificial neural network is instead an adaptive system that changes its structure based on external or internal information that flows through the network during the learning phase. In practical terms neural networks are nonlinear structures of statistical data organized as modeling tools. They can be used to simulate complex relationships between inputs and outputs that other analytic functions fail to represent. The SVM (Support Vector Machine) finally are a set of supervised learning methods used for classification. Given a set of training examples, each marked as belonging to two possible categories, a training SVM algorithm builds a model that can predict which category must be from a new sample input.

What is usually done is to collect a large series and classify them according to clinical experience in at least two classes (the sick and the healthy). Cutting across this division we shall proceed to divide the set into two groups the first of which will be used to train the expert system and the second to assess the performance of the classifier: the choice of cases to be used in the training set and the control set must be random, but the number and the ratio of cases to be used is a key parameter for the success of the training. The choice of parameters which will serve as input to the system is an essential step and requires experience and sensitivity.

The only drawback to this approach is that of a priori classification frameworks: as there is no fixed rule for the certainty of keratoconus and being the interpretation of the clinical frameworks still too arbitrary such arbitrariness is reflected in what the expert system learns, in a much stronger way when the diagnosis of keratoconus is precocious. In fact, the more prematurely topographers are able to read signs of ectasia the less agreement there will be on the interpretation of signs and classification.

Compliance with Ethical Requirements *Conflict of Interest*: Francesco Versaci and Gabriele Vestri are employees of CSO srl.

Informed Consent: No human studies were carried out by the authors for this article.

Animal Studies: No animal studies were carried out by the authors for this article.

References

1. Jongsma FHM, De Brabander J, Hendrikse F. Review and classification of corneal topographers. Lasers Med Sci. 1999;14(1):2–19.
2. Mejía-Barbosa Y, Malacara-Hernández D. A review of methods for measuring corneal topography. Optom Vis Sci. 2001;78(4):240–53.
3. Atchison DA, Smith G. Optics of the human eye. Oxford: Butterworth-Heinemann; 2000. p. 34–5.
4. von Helmholtz H. Graefe's Archiv für Ophthalmologie. 1854;2:3.

5. Wilson SE, Wang J-Y, Klyce SD. Quantification and mathematical analysis of photokeratoscopic images. In: Shanzlin DJ, Robin JB, editors. Corneal topography. New York: Springer; 1992. p. 1–9.
6. Klyce SD. Computer-assisted corneal topography. High-resolution graphic presentation and analysis of keratoscopy. Invest Ophthalmol Vis Sci. 1984;25(12): 1426–35.
7. Doss JD, et al. Method for calculation of corneal profile and power distribution. Arch Ophthalmol. 1981;99(7):1261–5.
8. van Saarloos PP, Constable IJ. Improved method for calculation of corneal topography for any photokeratoscope geometry. Optom Vis Sci. 1991;68(12):960–65.
9. Campbell C. Reconstruction of the corneal shape with the mastervue Corneal Topography System. Optom Vis Sci. 1997;74(11):899–905.
10. Mattioli R, Tripoli NK. Corneal geometry reconstruction with the Keratron videokeratographer. Optom Vis Sci. 1997;74(11):881–94.
11. Klein SA. Axial curvature and the skew ray error in corneal topography. Optom Vis Sci. 1997;74(11):931–44.
12. Merklinger HM. Focusing the view camera. Bedford: Seaboard Printing Limited; 1996. p. 5.
13. Izatt JA, et al. Micrometer-scale resolution imaging of the anterior eye in vivo with optical coherence tomography. Arch Ophthalmol. 1994;112(12):1584–9.
14. Fercher AF, et al. In-vivo dual-beam optical coherence tomography. In: Europto Biomedical Optics' 93. International Society for Optics and Photonics. 1994.
15. Fercher AF, et al. Measurement of intraocular distances by backscattering spectral interferometry. Opt Commun. 1995;117(1):43–8.
16. Huang D, et al. Optical coherence tomography. Science. 1991;254(5035):1178–81.
17. Swanson EA, et al. In vivo retinal imaging by optical coherence tomography. Opt Lett. 1993;18(21):1864–6.
18. Drexler W, et al. Ultrahigh-resolution ophthalmic optical coherence tomography. Nat Med. 2001;7(4):502–7.
19. Chinn SR, Swanson EA, Fujimoto JG. Optical coherence tomography using a frequency-tunable optical source. Opt Lett. 1997;22(5):340–2.
20. Rabinowitz YS. Videokeratographic indices to aid in screening for keratoconus. J Refract Surg. 1995;11(5):371.
21. Rabinowitz YS, Mcdonnell PJ. Computer-assisted corneal topography in keratoconus. Refract Cor Surg. 1988;5(6):400–8.
22. Rabinowitz YS, Rasheed K. KISA% index: a quantitative videokeratography algorithm embodying minimal topographic criteria for diagnosing keratoconus. J Cataract Refract Surg. 1999;25(10):1327–35.
23. Mahmoud AM, et al. CLMI the cone location and magnitude index. Cornea. 2008;27(4):480.
24. Maeda N, et al. Automated keratoconus screening with corneal topography analysis. Invest Ophthalmol Vis Sci. 1994;35(6):2749–57.
25. Maeda N, Klyce SD, Smolek MK. Neural network classification of corneal topography. Preliminary demonstration. Invest Ophthalmol Vis Sci. 1995;36(7):1327–35.
26. Calossi A. Screening by computerized videokeratography [in Italian]. In: Il Cheratocono. Canelli: SOI Publishing Group, Fabiano Group Ltd; 2004. p.114–7.
27. Schwiegerling J, Greivenkamp JE. Keratoconus detection based on videokeratoscopic height data. Optom Vis Sci. 1996;73(12):721–8.
28. Langenbucher A, et al. [Keratoconus screening with wave-front parameters based on topography height data]. Klin Monbl Augenheilkd. 1999;214(4):217–23.
29. Ambrósio R, et al. Corneal-thickness spatial profile and corneal-volume distribution: tomographic indices to detect keratoconus. J Cataract Refract Surg. 2006;32(11):1851–9.
30. Piñero DP, et al. Corneal volume, pachymetry, and correlation of anterior and posterior corneal shape in subclinical and different stages of clinical keratoconus. J Cataract Refract Surg. 2010;36(5):814–25.
31. Uçakhan ÖÖ, et al. Evaluation of Scheimpflug imaging parameters in subclinical keratoconus, keratoconus, and normal eyes. J Cataract Refract Surg. 2011;37(6):1116–24.
32. Chastang PJ, et al. Automated keratoconus detection using the EyeSys videokeratoscope. J Cataract Refract Surg. 2000;26(5):675–83.
33. Arbelaez MC, et al. Use of a support vector machine for keratoconus and subclinical keratoconus detection by topographic and tomographic data. Ophthalmology. 2012;119(11):2231–38.
34. Cortes C, Vapnik V. Support-vector networks. Mach Learn. 1995;20(3):273–97.
35. Cristianini N, Shawe-Taylor J. An introduction to support vector machines and other kernel-based learning methods. Cambridge: Cambridge University Press; 2000.